

1 **Holocene palaeoenvironmental changes in the Thar Desert: an integrated**
2 **assessment incorporating new insights from aeolian systems**

3 Aayush Srivastava^{a*}, David S.G. Thomas^{a,b}, Julie A. Durcan^a and Richard M. Bailey^a

4 ^a School of Geography and the Environment, University of Oxford, Oxford, OX1 3QY,
5 United Kingdom

6 ^b School of Geography, Archaeology and Environmental Studies, University of the
7 Witwatersrand, Johannesburg 2050, South Africa

8 *Corresponding author

9 E-mail: aayush.srivastava@ouce.ox.ac.uk (A. Srivastava)

10

11 **Abstract**

12 Due to the scarcity of geochemical and palaeoecological proxies in drylands, dunes
13 have often been used as geoproxies for late Quaternary palaeoenvironmental
14 reconstruction, with chronologies commonly provided by luminescence dating.
15 Owing to their widespread occurrence and location in a monsoonal regime, dunes in
16 the Thar Desert in South Asia act as important archives of past landscape change.
17 Previous reviews have assimilated dune age data from the Thar and suggested a
18 temporally and spatially complex record of sediment accumulation over the last ~70
19 ka. New luminescence age data presented in this study and from recent dunefield
20 based investigations demonstrate a stronger Holocene record of dune building in
21 parts of the Thar than previously suggested.

22 In this study, the Accumulation Intensity (*AI*) methodology is applied to new and old
23 data sets, providing records of dune accumulation that can be analysed alongside

24 other palaeoenvironmental records. *AI* analysis demonstrates the significance of
25 Holocene dune accumulation in the Thar landscape, with accumulation peaks
26 observed between ~12 and ~8 ka, centred around ~7, ~5 and ~3.5 ka, and in last
27 two millennia. The strengthening of the Indian Summer Monsoon remains a
28 significant influence on widespread dune accumulation in the early Holocene, but
29 dunefields have also shown diverse and spatially intensive responses to sediment
30 supply and anthropogenic disturbances during the late Holocene. Additionally,
31 aeolian-fluvial sequences associated with the Ghaggar-Hakra palaeochannel along
32 the northern margin of the Thar also display dynamic geomorphic behaviour during
33 the Holocene. The integration and interpretation of the *AI* data with published, highly
34 resolved geochemical proxies of palaeoclimate, shows a complex relationship
35 between geoproxy and geochemical records. We suggest that process studies of
36 geomorphologic systems and their diverse responses to the same environmental
37 stimuli must be given due consideration before deriving palaeoenvironmental
38 interpretations. Despite the presence of over a hundred Holocene dune records from
39 the Thar, there still remains marked spatial and temporal gaps. Further intensive
40 investigations of distinct dunefields with a strong chronometric framework and
41 geomorphological grasp are required to gain significant insights into wider Thar
42 landscape and palaeoenvironmental dynamics.

43 *Keywords: Thar Desert, Holocene; Dune accumulation; Accumulation Intensity;*
44 *palaeoenvironmental change*

45

46

47

48 **1. Introduction**

49 The landscape of the Thar Desert in South Asia is dominated by sand dunes of
50 different types including parabolic, linear, and transverse, of up to 30 m in height
51 (Kar, 1993; Singhvi and Kar, 2004; Moharana et al., 2013). These features have long
52 been viewed as offering insights into landscape and climate change during the
53 Quaternary period. Based on dune orientation, earlier studies proposed a dominant
54 role of south-westerly Indian Summer Monsoon (ISM) winds in dune development in
55 the Thar (e.g. Goudie et al., 1973; Allchin et al., 1978; Wasson et al., 1983; Kar,
56 1987). The ISM winds, based on meteorological observations, have been shown to
57 exceed the threshold for sand movement in the pre-monsoon period (March to June)
58 before the onset of rainfall (Wasson et al., 1983; Kar, 1993). Aeolian activity is strong
59 during this period when vegetation is dry, and wind erosion of the terrain and
60 subsequent sediment transportation and deposition are more pronounced (Wasson
61 et al., 1983; Kar, 1993). It is only after this period of increased wind intensity that
62 precipitation (~80% of the total annual amount) is delivered to the region, between
63 the months of June and September, resulting in positive precipitation minus
64 evaporation conditions. Therefore, whilst periods of more intensive monsoon activity
65 can be associated with increased precipitation, they can also represent phases of
66 more intensive aeolian activity. However, there was an absence of temporal control
67 on Thar dune development until Singhvi et al. (1982) used thermoluminescence (TL)
68 dating to provide the first chronometric perspective, with eight ages calculated from
69 three dune sites. Since then over 150 dune samples in the Thar have been
70 investigated and dated using both TL and optically stimulated luminescence (OSL)
71 dating techniques (e.g. Andrews et al., 1998; Kar et al., 1998; Thomas et al., 1999;
72 Kar et al., 2001; Juyal et al., 2003). Singhvi and Kar (2004) summarised these

73 investigations and concluded these records provide a first-level understanding of
74 aeolian episodes in the Thar, with Singhvi and Porat (2008) further assessing and
75 briefly summarising key results from the Thar dunefield age data. Lancaster et al.
76 (2016) collated all the Thar dune luminescence ages published in peer reviewed
77 studies (>150) in the INQUA dune atlas chronologic database.

78 Despite a relatively large published luminescence age data set, the interrogation of
79 the Thar dune records in the context of understanding past landscape dynamics has
80 been challenging. The aeolian records need to be assessed alongside other proxy
81 data if environmental dynamics and their drivers are to be determined. Two main
82 reasons explain the challenges that have occurred. First, there has been a lack of
83 spatial and temporal coverage in the available aeolian data set until recently, as
84 shown in Figure 1. For instance, the central Thar dune record was represented by
85 just three Holocene ages from two sites, Chamu and Shergarh Trijunction (Andrews
86 et al., 1998; Dhir et al., 2010). In contrast, the southern and northern Thar areas
87 were the subject of several dune-based investigations, which identified major early
88 and late Holocene dune accumulation phases respectively (Figure 1b).
89 Consequently, single dune sites were often considered representative of the wider
90 region, although they inevitably failed to capture dunefield development history and
91 inhibited analyses of the drivers of dune accumulation. Recent dunefield based
92 studies by Srivastava et al. (2019a; 2019b) have revealed significant Holocene
93 aeolian accumulation, and presented 50 new OSL ages from a mixture of parabolic
94 and linear dunes, demonstrating that dune accumulation was persistent throughout
95 much of the Holocene, adding a significant late Holocene data set which was
96 infrequently identified in earlier studies. Second, it has been difficult to integrate the
97 aeolian age records, which have been discontinuous with other proxy records, an

98 issue observed in other dryland contexts worldwide (Thomas and Bailey, 2017).
99 Therefore, reconstructions of Holocene palaeoenvironments in the Thar rely on other
100 terrestrial archives including fluvial records from the Thar margins (e.g. Jain and
101 Tandon, 2003; Jain et al., 2004; Giosan et al., 2012; Durcan et al., 2019), and
102 lacustrine sediments from various interior and marginal lakes (e.g. Wasson et al.,
103 1984; Singh et al., 1990; Kajale and Deotare, 1997; Enzel et al., 1999; Deotare et al.,
104 2004; Sinha et al., 2006; Dixit et al., 2014a; Dixit et al., 2014b; Dixit et al., 2018)
105 These records are often supplemented by regional palaeoclimatic proxies, including
106 sedimentary and productivity records from marine sediments (e.g. Sarkar et al., 2000;
107 Staubwasser et al. 2002; Gupta et al., 2003; Ivanochko et al., 2005; Ponton et al.,
108 2012) and isotopic records from speleothems in central or north-eastern India (Sinha
109 et al., 2007; Sinha et al., 2011a; Dutt et al., 2015; Berkelhammer et al., 2012; Band
110 et al., 2018) and the Arabian peninsula (e.g. Neff et al., 2001; Fleitmann et al., 2003;
111 Fleitmann et al., 2007) (Figure 2). These records present high resolution data, but
112 due to their limited spatial context, diverse methodologies and different temporal
113 ranges, landscape scale response interpretations arising from these geochemical
114 proxies are often conflicting in nature (e.g. Prasad and Enzel, 2006; Macdonald,
115 2011, Band et al., 2018; Kaushal et al., 2018; Misra et al., 2019). Dunes, whilst
116 widespread in the Thar landscape, remain under-utilised in environmental
117 reconstructions, representing a valuable archive of change.

118 In the context of these considerations, this paper aims first to systematically analyse
119 the both new and existing dune age data set from the Thar Desert using the
120 numerical Accumulation Intensity (*AI*) analysis approach of Thomas and Bailey
121 (2017; 2019). Then, focussing on the Holocene, the dune accumulation records are
122 assessed alongside other published proxy data sets to re-evaluate landscape

123 dynamics and change in the Thar. Finally, the new analysis is assessed in terms of
124 potential drivers of climate, along with consideration of data gaps and issues within
125 the existing portfolio of dune records.

126 **2. Accumulation Intensity modelling**

127 Several studies have highlighted difficulties in using dune age records in
128 palaeoenvironmental and paleoclimate analyses. These difficulties include sampling
129 issues (Hesse, 2016), taphonomic issues related to reworking of sediments (Bailey
130 and Thomas, 2014), data presentation issues (Thomas and Burrough, 2012; Thomas
131 and Burrough, 2016), and the definitive identification of controls on dune sediment
132 transportation (Chase, 2009). To address these issues, Bailey and Thomas (2014)
133 first developed the dune Accumulation Rate Variability model, identifying and
134 quantifying the drivers of dune accumulation. This was subsequently modified to the
135 *AI* model which utilises information on the actual sedimentation process in dunes to
136 produce temporal *AI* curves through time, which can be compared with other
137 palaeoenvironmental proxy data sets (Thomas and Bailey, 2017). In principle, the
138 model integrates and analyses central ages, their associated one sigma
139 uncertainties, and sampling interval depth data, and then iteratively resamples these
140 ages (within their uncertainties) to calculate accumulation rates. The dispersion in
141 the resampled accumulation rates acts as a proxy for the estimated accumulation
142 rate (Thomas and Bailey, 2017; 2019). Full mathematical detail of the model is
143 explained in Thomas and Bailey (2017).

144 The model has several advantages. It calculates temporal changes in dune
145 accumulation through time, independent of the number of samples included in the
146 analysis, allowing the retrieval of continuous palaeoenvironmental information from

147 dated dune sequences. Further, as the model incorporates age certainties into
148 analyses, any apparent age inversions are handled appropriately. The *AI* method is
149 applied to data from dunefields rather than individual dunes, and hence allows a
150 more systematic testing of landscape-scale responses and relationships to external
151 drivers at global and regional scales.

152 The model has been successfully used to compare and explain dunefield
153 accumulation histories in the context of other deserts in southern Africa and Australia
154 in conjunction with other continental and marine records (Thomas and Bailey, 2017).
155 Recently, Thomas and Bailey (2019) applied the *AI* methodology to the Asian dune
156 age data sets included in the INQUA dune atlas (Lancaster et al., 2016), focusing on
157 the last 50 ka, including the records for the Thar. The authors highlighted the
158 shortage of paired stratigraphically related ages from investigated dune sections and
159 absence of locational/depth data. The resultant *AI* curve was therefore noted for its
160 relatively limited spatial coverage, as well as containing insufficient data to provide a
161 nuanced assessment of Thar dune accumulation in the late Quaternary. This paper
162 addresses this shortfall by incorporating recently published age records into a new *AI*
163 analysis.

164 ***2.1 Data included in AI analysis***

165 There were 146 Thar dune luminescence ages in the first version of the INQUA dune
166 atlas database (Lancaster et al., 2016), which after updates, now includes a further
167 26 ages from Shitaoka et al (2012) and Durcan et al (2019). Recent studies have
168 expanded the available luminescence age data set by providing 50 new dune ages
169 (Srivastava et al., 2019a; Srivastava et al., 2019b) from the central and northern
170 Thar.

171 In addition to these published ages, 10 new dune accumulation records from
172 parabolic dunes in the central Thar and from a source-bordering dune associated
173 with the Ghaggar-Hakra palaeochannel in the north have been determined and are
174 included in this study. These new OSL ages, from the early to middle Holocene,
175 have been determined using small aliquots of coarse quartz grains (180-210 μm)
176 following the luminescence dating methods outlined in Srivastava et al. (2019a)
177 (Table 1). The full details regarding sampling and luminescence dating results are
178 provided in the Supplementary Information. Figure 1 displays the full set of available
179 luminescence Holocene records from the database and new studies, categorised in
180 four regions: northern, central and southern Thar, and Ghaggar-Hakra
181 palaeochannel following geographical contexts described in original publications.

182 This combined data set for the Thar provides an opportunity to enhance the spatial
183 and temporal detail of dune accumulation, to the point where Thar dune data can
184 contribute more robustly to palaeoenvironmental analyses for the region. The full
185 data set for this new *AI* analysis, using the methodology of Thomas and Bailey
186 (2017), therefore comprises (see Supplementary Information for details of all
187 records):

- 188 1. 73 dune ages, generating 59 accumulation intervals, from a total of 146 ages
189 presented in the database from sites Thirana, Jamsar (Thomas et al., 1999),
190 Chamu (Dhir et al., 2010), Amarsar (Singhvi and Kar, 2004), Dharoi (Juyal et
191 al., 2003) and Khudala (Thomas et al., 1999; Kar et al., 2001). Many ages did
192 not meet the required criteria for *AI* analysis due to an absence of locational
193 or depth data, or the occurrence of age reversals which meant net
194 accumulation could not be identified (Thomas and Bailey, 2017). Further,
195 ages from mobile transverse dunes (e.g. Khara, Bharmasar; Figure1; Kar et

196 al., 1998) were excluded on the account of lower likelihood of sediment
197 preservation (Bailey and Thomas, 2014).

198

199 2. 83 of 86 newly published ages, from two dunefields in the central Thar
200 (Jodhpur; Srivastava et al., 2019b; this study) and the northern Thar (Bikaner;
201 Srivastava et al., 2019a), and aeolian sequences in Shitaoka et al. (2012) and
202 Durcan et al., (2019), generating 58 accumulation intervals.

203

204

205

206

207

208

209

210

211

212

213

214

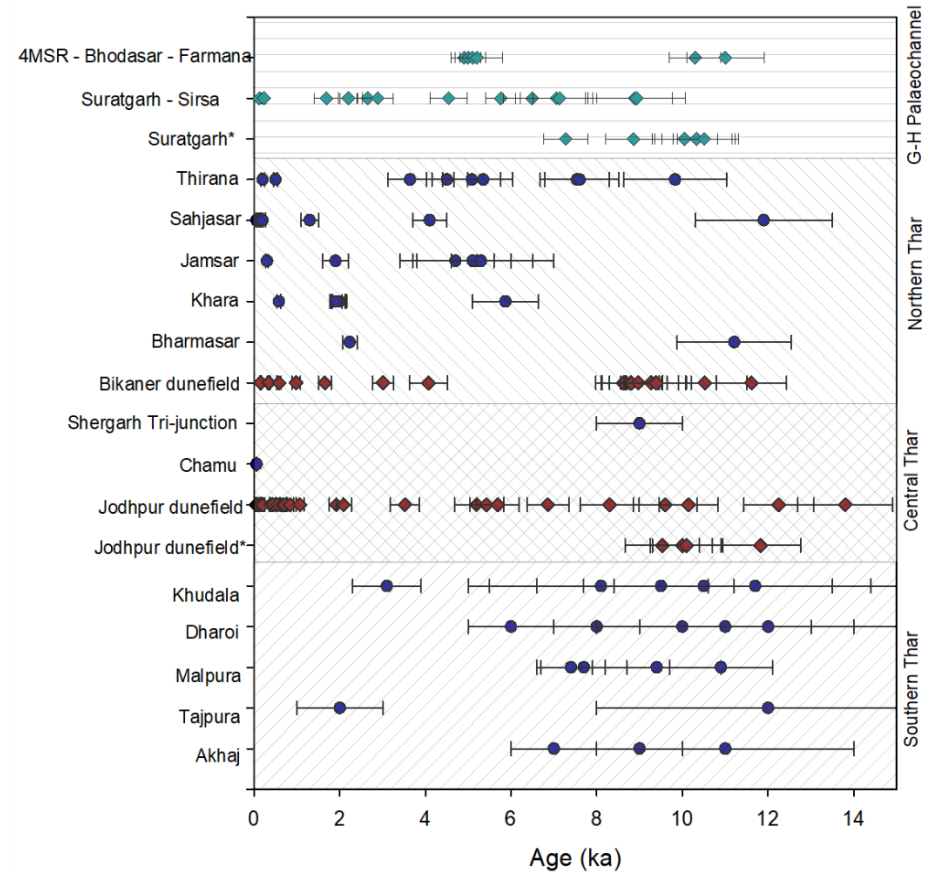
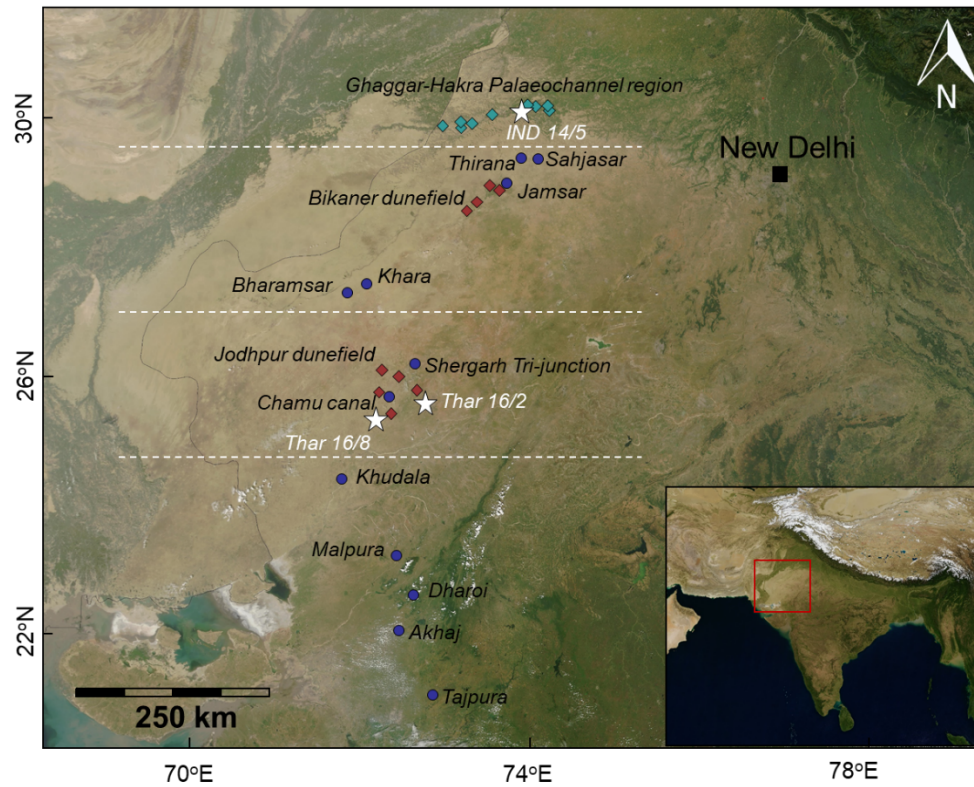
215

216

217

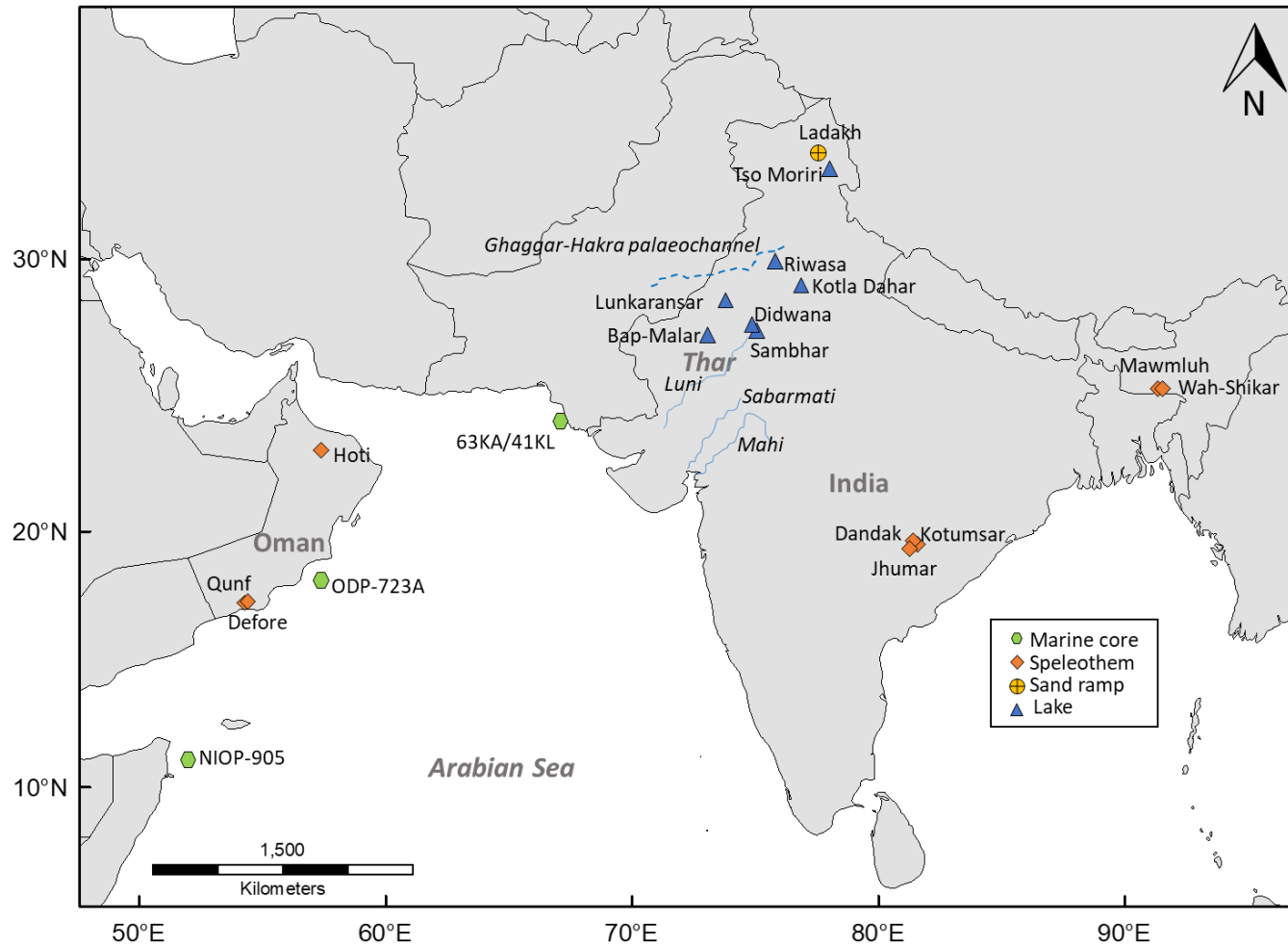
218 **Table 1. Summary OSL data of new ages included in this study. Equivalent doses (D_e), dose rates (\dot{D}), and ages are shown**
 219 **to two decimal places, with all calculations made prior to rounding. All ages were calculated using Central Age Model**
 220 **(CAM) and are relative to the year 2018.**

Sample	Depth (m)	Discs accepted (measured)	Overdispersion (%)	CAM D_e (Gy)	Beta \dot{D} (Gy.ka ⁻¹)	Gamma \dot{D} (Gy.ka ⁻¹)	Cosmic \dot{D} (Gy.ka ⁻¹)	Envir \dot{D} (Gy.ka ⁻¹)	Age (ka)
Thar 16/2/1	21	23 (50)	32.7 ± 4.3	24.55 ± 1.84	1.43 ± 0.11	1.12 ± 0.08	0.03 ± 0.02	2.58 ± 0.14	9.53 ± 0.87
Thar 16/2/3	22	23 (42)	26.7 ± 4.1	25.28 ± 1.43	1.25 ± 0.10	0.86 ± 0.06	0.03 ± 0.02	2.14 ± 0.12	11.83 ± 0.93
Thar 16/8/1	2	28 (48)	24.3 ± 3.5	21.82 ± 1.04	1.16 ± 0.09	0.86 ± 0.06	0.16 ± 0.02	2.18 ± 0.11	10.01 ± 0.70
Thar 16/8/2	3	23 (68)	31.9 ± 4.9	24.43 ± 1.66	1.33 ± 0.10	0.96 ± 0.06	0.14 ± 0.02	2.43 ± 0.13	10.04 ± 0.85
IND 14/5/1	2	20 (30)	21.8 ± 3.8	18.99 ± 0.97	1.43 ± 0.11	1.02 ± 0.07	0.16 ± 0.02	2.61 ± 0.13	7.28 ± 0.52
IND 14/5/2	3	20 (46)	22.4 ± 5.4	22.60 ± 1.21	1.42 ± 0.11	0.99 ± 0.07	0.14 ± 0.02	2.55 ± 0.13	8.86 ± 0.66
IND 14/5/3	10	34 (48)	22.6 ± 3.2	23.02 ± 0.96	1.31 ± 0.11	0.81 ± 0.05	0.07 ± 0.02	2.19 ± 0.13	10.51 ± 0.73
IND 14/5/4	11	18 (28)	12.6 ± 2.8	28.75 ± 1.01	1.48 ± 0.11	1.19 ± 0.08	0.06 ± 0.02	2.74 ± 0.14	10.51 ± 0.64
IND 14/5/5	25	29 (60)	28.8 ± 4.3	28.90 ± 1.65	1.54 ± 0.11	1.31 ± 0.09	0.02 ± 0.02	2.88 ± 0.14	10.05 ± 0.76
IND 14/5/6	26	18 (28)	30.0 ± 5.9	25.78 ± 2.04	1.41 ± 0.11	1.07 ± 0.07	0.02 ± 0.02	2.50 ± 0.13	10.33 ± 0.97



223 **Figure 1. (a) The locations of studied Holocene dune sites in the Thar. Blue circles denote sites as described in Singhvi**
 224 **and Kar (2004) and listed in the first version of the INQUA dune database (Lancaster et al., 2016): Thirana, Sahjasar,**

225 **Jamsar, Malpura (Thomas et al., 1999), Khara, Bharmasar (Kar et al., 1998), Chamu (Dhir et al., 2010), Khudala (Kar et al.,**
226 **2001), Dharoi, Tajpura and Akhaj (Juyal et al., 2003); red diamonds denote sites investigated in Bikaner dunefield in the**
227 **northern Thar (Srivastava et al, 2019a) and Jodhpur dunefield in the central Thar (Srivastava et al., 2019b); blue diamonds**
228 **denote sites along the Ghaggar-Hakra palaeochannel further along the northern Thar margin (Shitaoka et al., 2012; Durcan**
229 **et al., 2019), white stars represent new sites included in this paper (see Supplementary Information). (b) Associated**
230 **Holocene dune ages reported from the investigated sites. (*) represents the new ages presented in this study.**



231

232 **Figure 2. The locations of different types of proxy records from north-western India and beyond, as discussed in this**

233 **paper.**

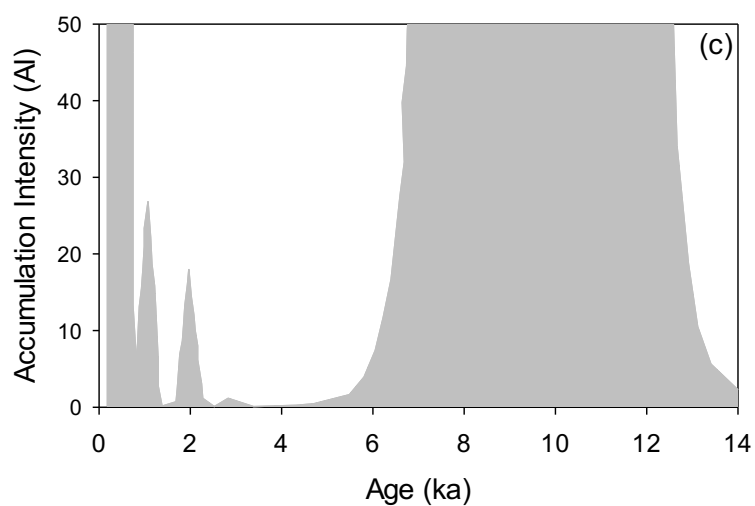
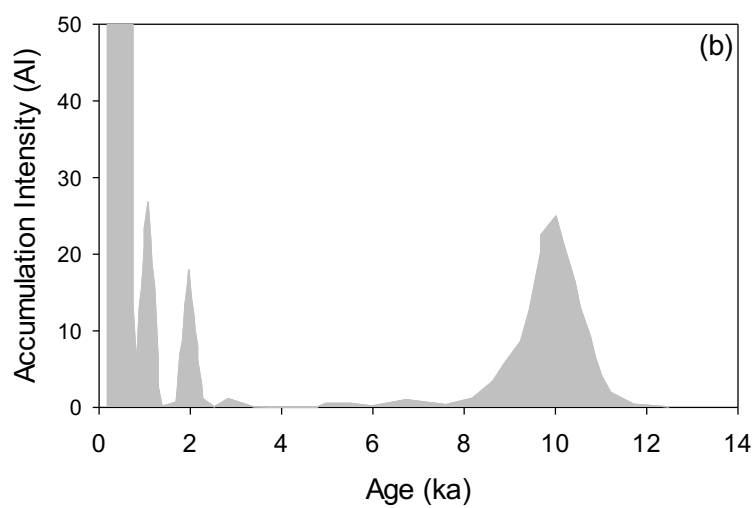
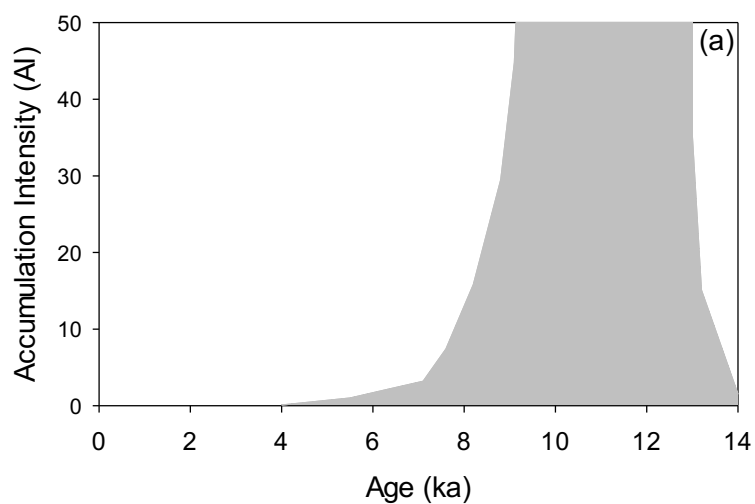
234 **2.2 A new *AI* record for the Thar Desert**

235 The new Holocene *AI* record for the Thar Desert is presented in Figure 3. For
236 contrast, Figure 3a shows the initial Thar *AI* plot from Thomas and Bailey (2019),
237 based only on the ages included in the original dune atlas database (Lancaster et al.,
238 2016). Figure 3b shows the *AI* plot from the recently published OSL ages from
239 parabolic and linear dunefields in the central and northern Thar (Srivastava et al.,
240 2019a; Srivastava et al., 2019b), aeolian sequences along the Ghaggar-Hakra
241 palaeochannel (e.g. Shitaoka et al., 2012; Durcan et al., 2019) and ten new OSL
242 ages presented in this study (Table 1). Figure 3c shows the integrated results of *AI*
243 analysis generated after combining all the Thar dune records included in Figure 3a
244 and 3b.

245 The broadest accumulation peak falls within the late Pleistocene and early to middle
246 Holocene period, extending from ~14 to ~6 ka based on >40 individual ages. The
247 breadth of the peak in Figure 3a and 3c occurs as a result of the larger age
248 uncertainties associated with the previously published ages, which are in the range ~
249 $\pm 10\text{-}40\%$ (Table S3). The new and recently published OSL ages (this study;
250 Srivastava et al., 2019a; Srivastava et al., 2019b) have lower uncertainties (less than
251 $\pm 10\%$), which when incorporated into the *AI* model results in a narrower
252 accumulation peak (Figure 3b). Thomas and Bailey (2017) discuss this in their paper,
253 commenting that as uncertainties increase, peak broadness increases and peaks
254 become less refined (see Figure 4A, 4B of Thomas and Bailey, 2017). Regardless of
255 the resolution, the early Holocene is a period of high aeolian accumulation in the
256 Thar Desert.

257 In the middle to late Holocene, as shown in Figure 3b, peaks are centred at ~7, ~5
258 and ~3.5 ka. Interestingly, there are no peaks or secondary 'shoulders' observed
259 between ~5 and ~3.5 ka despite the presence of six luminescence ages (Figure 1). It
260 can be explained in the context of underlying principles of *AI* analysis as these six
261 ages have been calculated from different sampling locations in the Thar and hence
262 associated accumulation thickness cannot be calculated. Another important
263 consideration is that due to nature of y axis resolution, sometimes minor rises may
264 not be displayed unless magnified (e.g. southern Kalahari dunefield; Thomas and
265 Bailey, 2017).

266 The late Holocene peaks are notably absent from the original analysis from dune
267 database records (Figure 3a). Prior to the recent application of intensive sampling
268 through full dune sediment profiles, studies tended to exclude the upper few metres
269 of dune sediments from investigation, sampling deeper sections, and therefore
270 potentially under-representing the late Holocene records. With the inclusion of new
271 data in this *AI* analysis, strong peaks appear in the late Holocene centred around ~2
272 ka and ~1 ka, with the most nuanced one based on 14 ages representing the last
273 two centuries. Unlike the early Holocene peaks, the late Holocene *AI* peaks increase
274 in size due to younger ages having narrower one sigma error ranges (causing
275 accumulation concentrated towards the central age) and probabilistic likelihood of
276 better preservation of younger accumulation phases (Bailey and Thomas, 2014).



277

278 **Figure 3. (a). Holocene AI plots for the Thar based on dune luminescence ages**
 279 **first listed in INQUA dune atlas database (Lancaster et al., 2016). (b). based on**

280 recent studies (Shitaoka et al., 2012; Durcan et al., 2019; Srivastava et al.,
281 2019a; Srivastava et al., 2019b; this study). (c). all combined.

282

283 3. Drivers of Thar landscape change during the Holocene

284 3.1 Early Holocene (~11.7 - ~8.2 ka)

285 As the Thar lies in a monsoonal regime, the ISM winds remain one of the major
286 drivers of dune accumulation in the desert (Wasson et al., 1983; Kar, 1993; Singhvi
287 and Kar, 2004; Srivastava et al., 2019a). As shown by the strongest peak in the *AI*
288 plot (Figure 3) and >30 individual luminescence ages from dunefields (Figure 1), the
289 Thar landscape experienced widespread dune accumulation during the early
290 Holocene. At least 3 parabolic dune sites in the central Thar and 4 linear dune sites
291 in the northern Thar have been shown to have recorded accumulation between 12.2
292 ± 0.8 ka and 8.7 ± 0.6 ka, with net dune accumulation up to 3.5 m per year
293 (Srivastava et al. 2019a; Srivastava et al. 2019b). The new ages presented in this
294 paper are also consistent with these published early Holocene records (Table 1).
295 The basal ages from a parabolic dune near Jodhpur (Thar 16/2; Figure 1) date to
296 9.53 ± 0.87 ka (Thar 16/2/1) and 11.83 ± 0.93 ka (Thar 16/2/3). The samples
297 investigated from another parabolic dune Thar 16/8 also display consistency and
298 further give evidence of an early Holocene dune accumulation between 10.01 ± 0.70
299 ka (Thar 16/8/1) and 10.04 ± 0.85 ka (Thar 16/8/2). Dunes at the northern margin of
300 the Thar, associated with the Ghaggar-Hakra palaeochannel system, also record
301 early Holocene aeolian accumulation. Six samples from one such source-bordering
302 dune in the northern Thar margin show a rapid ~16 m thick dune accumulation
303 between 10.05 ± 0.76 ka and 10.51 ± 0.73 ka (site IND 14/5; Table 1). The shallower

304 samples at this site record dune activity at 7.28 ± 0.52 ka and 8.86 ± 0.66 ka at
305 depths of 2 and 3 m (Table 1). Shitaoka et al. (2012) and Maemoku et al. (2012)
306 dated sediments from nearby dunes to report accumulation between ~15-10 ka,
307 however, the extent of accumulation cannot be compared because their studies are
308 based on ≤ 2 samples from each dune. From the same area, Durcan et al. (2019),
309 also used OSL dating to report aeolian accumulation dating to 8.93 ± 1.14 ka at 0.5
310 m and 8.89 ± 0.88 ka from uppermost 3.3 m of a dune in the same dunefield.
311 Further to the north in the cold desert of Ladakh, Kumar et al. (2017) investigated
312 five sand ramps using sedimentology and OSL dating and identified a phase of
313 persistent high sedimentation rate between ~12 and ~8 ka. In the southern Thar,
314 fluvial records from the Luni River suggest incision during this phase, which was
315 followed by sheet flow aggradation between ~9 and ~5 ka (Jain and Tandon, 2003).
316 Further south, records from the perennial Mahi and Sabarmati Rivers also indicate
317 that these rivers incised during the early Holocene primarily governed by accelerated
318 fluvial activity and large runoff as a response to enhanced ISM (Srivastava et al.,
319 2001; Jain and Tandon, 2003; Jain et al., 2004).

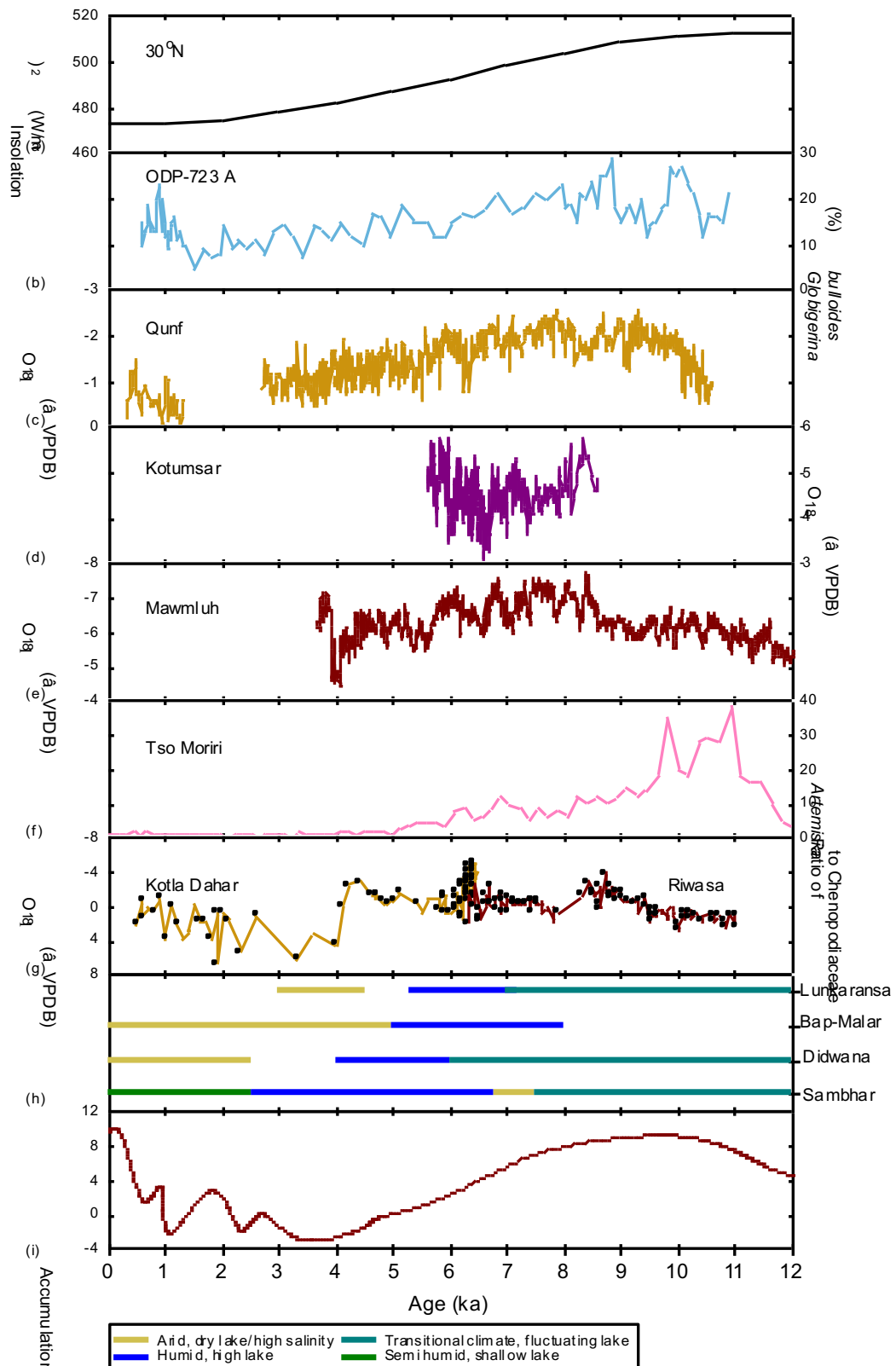
320 The strong *Al* peaks, consistent with thick dune accumulation records from the Thar
321 and beyond attest to a wider dynamic landscape response in the early Holocene.
322 This period was marked by precessionally forced changes in insolation resulting in
323 the intensification of the monsoon systems (Berger and Loutre, 1999; Wang et al.,
324 2005), as evidenced in an array of terrestrial and marine proxies. In terrestrial
325 records from north-western India, a $\delta^{18}\text{O}$ study conducted on ostracods from
326 palaeolake Riwasa sediments (Figure 4) by Dixit et al. (2014b) showed that lake
327 levels were high between ~9.4 and ~8.3 ka, in concurrence with the early Holocene
328 monsoon strengthening. The other lakes in the Thar (notably Sambhar, Didwana,

329 Bap-Malar and Lunkaransar), however, show differences in the onset timings of
330 fluctuations in levels and salinity throughout the Holocene (Figure 4). Lake level
331 peaks do not directly correlate with the early Holocene ISM strength, as the high lake
332 levels were reported to have occurred in the middle Holocene (Prasad and Enzel,
333 2006; Macdonald, 2011; Misra et al., 2019). Furthermore, Lake Sambhar in the
334 eastern Thar does not record any evidence of complete desiccation (Sinha et al.,
335 2006). These differences, which highlight the difficulties in considering individual lake
336 records as representative of the regional picture, may be due to a multitude of
337 reasons including differences in their geographic locations and groundwater
338 discharges, resulting in different hydrological responses to rainfall changes as well
339 as basin size, depth and morphology (e.g. Bowler, 1986); differences in the proxy
340 records analysed in individual studies resulting in diverse interpretations (e.g.
341 Burrough and Thomas, 2009); differences in employed dating methods and
342 interpretive resolutions (e.g. Cohen, 2003) and finally the additional possibility of
343 winter rainfall also contributing to the hydrology of some of the basins (Enzel et al.,
344 1999; Prasad and Enzel, 2006).

345 The published Holocene speleothem records are scarce within the peripheral domain
346 of the ISM in the Indian subcontinent and do not often cover the entire Holocene
347 period (e.g. Yadava and Ramesh, 1999; Dixit and Tandon, 2016; Kaushal et al.,
348 2018; Band et al., 2018 and references therein). Nevertheless, more negative $\delta^{18}\text{O}$
349 values reported from speleothem records in the Mawmluh Cave, north-eastern India
350 suggest an enhanced ISM precipitation in the early Holocene (Berkelhammer et al.,
351 2015; Dutt et al., 2015). The other high-resolution $\delta^{18}\text{O}$ records from speleothems in
352 Oman also indicate a rapid increase in ISM strength between ~ 10.6 and ~ 9.7 ka in
353 southern Oman (Qunf and Defore Caves) and between ~ 10.1 and ~ 9.2 ka in

354 northern Oman (Hoti Cave) (Figure 4; Fleitmann et al., 2003; Fleitmann et al., 2007)
355 which is consistent with widespread early Holocene dune accumulation in the Thar.
356 Holocene ISM variability has been inferred from the Arabian Sea sedimentary
357 records as the region experiences upwelling driven by this monsoon system. Gupta
358 et al. (2003) presented a high-resolution foraminifer (*Globigerina bulloides*)
359 productivity record of wind strength from a core off the coast of Oman (ODP- 723).
360 This suggested an early Holocene strengthening of the ISM marked by discrete
361 weak intervals (Figure 4). Another productivity record based on *Neogloboquadrina*
362 *dutertrei* from south-western Arabia Sea core NIOP-905 also shows broad
363 consistency with Gupta et al. (2003)'s observations (Ivanochko et al., 2005).
364 Staubwasser et al. (2002) presented a record of the Indus River discharge using
365 *Globigerinoides ruber* $\delta^{18}\text{O}$ from core 63KA/41KL off Pakistan, and suggested
366 strengthening of the ISM between ~12 and 11 ka BP with maximum Indus water
367 discharge at ~9.4 ka. Gill et al. (2017) hypothesised teleconnections from the Pacific
368 and based on sea surface temperature proxies from 27 locations scattered across
369 the equatorial Pacific revealed the greatest ISM wind stress curl during this period.
370 The correlation between upwelling and wind strength proxies from the Arabian Sea
371 and enhanced phases of dune accumulation thus most likely suggest an in-phase
372 relationship between general intensification of the ISM and dune accumulation in the
373 early Holocene.

374



375

376 **Figure 4. (a). Summer insolation (W/m^2) at $30^\circ N$ (from Berger and Loutre, 1999).**

377 **(b). *G. bulloides* percentage from a marine core ODP-723A off Oman (Gupta et**

378 al., 2003). (c). $\delta^{18}\text{O}$ record (‰ Vienna Peedee belemnite; VPDB) from a
379 stalagmite in the Qunf Cave, southern Oman (Fleitmann et al., 2003). (d). $\delta^{18}\text{O}$
380 record (‰ VPDB) from the Kotumsar Cave, central India (Band et al., 2018). (e).
381 $\delta^{18}\text{O}$ record (‰ VPDB) from the Mawmluh Cave, north-eastern India
382 (Berkelhammer et al., 2012). (f) pollen percentage ratio of *Artemisia* to
383 *Chenopodiaceae* (A/C) from Tso Moriri (Leipe et al., 2014) (g). Gastropod $\delta^{18}\text{O}$
384 record (‰ VPDB) from palaeolakes Kotla Dahar (Dixit et al., 2014a) and Riwasa
385 (Dixit et al., 2014b). (h) Schematic representation of Holocene
386 palaeolimnological history of four inland lakes in the Thar (Wasson et al., 1984;
387 Kajale and Deotare, 1997; Deotare et al., 1998; Enzel et al., 1999; Sinha et al.,
388 2006); (i) Summary *AI* curve for the Thar dune records as analysed in this
389 study.

390

391 **3.2 Middle Holocene (~8 - ~4.2 ka)**

392 The middle Holocene, in contrast to the early Holocene, has fewer records of dune
393 accumulation which come from scattered sites. In the *AI* plots, this period has
394 therefore fewer and more minor peaks (Figure 3c). As shown in Figure 1b there is a
395 relative lull in recorded dune accumulation between ~8.5 ka and ~7 ka in the
396 northern and central Thar, although there are luminescence ages from dune sites in
397 the southern Thar that show evidence of dune accumulation (Singhvi and Kar, 2004).
398 Juyal et al. (2003) associated southern Thar dune activity with the availability of
399 sediment from a large alluvial plain of regional rivers, notably the Mahi and the
400 Sabarmati, in combination with lower sea-levels, increasing sediment availability to
401 the wind, resulting in source-proximal dune accumulation despite the weaker ISM.

402 Several high-resolution records have suggested variability in ISM strength during the
403 middle Holocene (Gupta et al., 2003; Wang et al., 2005; Dixit et al., 2014a). Based
404 on stalagmite $\delta^{18}\text{O}$ records from the Kotumsar Cave in central India, Band et al.
405 (2018) showed that the intensity of ISM gradually declined between ~ 8.5 ka and ~ 6.5
406 ka, which was followed by a steady increase between ~ 6.3 and ~ 5.6 ka (Figure 4).
407 The brief period of re-intensification can also be observed in $\delta^{18}\text{O}$ records from other
408 Qunf and Mawmluh Caves (Fleitmann et al., 2003; Berkelhammer et al., 2012;
409 Figure 4). There are two dune sites in the northern (Jamsar) and central (Jodhpur)
410 Thar where dune accumulation was recorded in this phase, as reflected in the form
411 of minor *A/* peak in Figure 3b. Other geochemical records indicate further weakening
412 of the ISM after ~ 5 ka as evidenced from high $\delta^{18}\text{O}$ values in Kotla Dahar palaeolake
413 along the northern Thar margin (Dixit et al., 2014a; Figure 4), low *Artemisia* to
414 *Chenopodiaceae* pollen ratios from Tso Moriri Lake in northern India (Leipe et al.,
415 2014; Figure 4) and higher $\delta^{18}\text{O}$ values in speleothem record from Mawmluh in
416 north-eastern India (Berkelhammer et al., 2012; Figure 4). Despite a relatively
417 weaker ISM, dune accumulation is recorded along the Thar's north-eastern fringe
418 during the middle Holocene, coincident with enhanced fluvial activity. Saini and
419 Mujtaba (2010) and Durcan et al. (2019) dated silty sand fluvial sediments from the
420 Ghaggar-Hakra palaeochannel and reported fluvial deposition during this phase
421 which continued to ~ 4 ka. Multiple source bordering dunes in the vicinity, also
422 recorded dune activity (Shitaoka et al., 2012; Maemuku et al., 2012). Durcan et al.
423 (2019) suggested this concurrence of dune and fluvial activity to be related to
424 changing hydrological conditions of the palaeochannel, with the drying of the fluvial
425 system resulting an increase of sediment supply available for entrainment. They
426 hypothesised that dune accumulations on the floodplain of the Ghaggar-Hakra

427 channel are sourced from reworking of the fluvial sediments. Similar co-occurrence
428 has been shown in the context of landscape dynamics near Cooper Creek in the
429 Lake Eyre basin in central Australia where dune activity on the floodplain has direct
430 sediment influx from the fluvial system (Cohen et al., 2010; Maroulis et al., 2007).
431 Based on these data, it is evident that dune accumulation occurred over a large area
432 of the Thar Desert and its margins during the middle Holocene, attributable to
433 enhanced sediment supply from ephemeral fluvial channels set against the backdrop
434 of a weakening ISM. Further the coeval fluvial activity records suggest that during
435 the middle to late Holocene, the landscape along the Ghaggar-Hakra palaeochannel
436 possibly acquired a state of balance, which Li and Coulthard (2015) describe as a
437 geomorphic setting where both fluvial and aeolian processes operate together.

438 The middle Holocene palaeolimnological histories of the Thar lakes have often been
439 compared with the timing of dune accumulation to test a potential relationship. For
440 instance, Thomas et al. (1999) studied a palaeolake in the northern Thar (near
441 Jamsar) and hypothesised antiphase behaviour between dune accumulation and
442 lake aridity at ~5 ka that during a period of relatively increased aridity, lake dried up
443 which facilitated sand mobilisation. Prasad and Enzel (2006) also compared the
444 middle Holocene 'dune formation' episodes in the southern Thar with aridity records
445 from nearby lakes and suggested further analyses of the available regional climate
446 record. However, establishing any such relationship requires careful assessment of
447 each geomorphic system individually and their response to external factors. For
448 example, lakes that are groundwater or distant-catchment fed could be wet in
449 locations where dunes are also active (accumulating), as the forcing factors (local
450 wind /aridity, distant moisture source) do not conflict as evidenced in the case of
451 dunes and lakes in Badain Jaran Desert, Inner Mongolia, China (Yang et al., 2003;

452 Yang et al., 2010). Further, dunes can be active, and lakes wet over annual/decadal
453 cycles in regions with strongly seasonal climates, which is a characteristic of
454 monsoon environments such as the Thar. For instance, when Lake Bap-Malar
455 recorded high levels between ~8 ka and ~5 ka (Kajale and Deotare, 1997) (Figure 4),
456 parabolic dunes in the nearby dunefield (Srivastava et al., 2019b) were also
457 accumulating during the period. Therefore, a complex, nonlinear relationship should
458 be expected between lake hydrological changes and dune records.

459

460 **3.3 Late Holocene (~4.2 ka - ~present)**

461 In the late Holocene, two minor peaks are observed between ~3.5 ka and ~1.5 ka
462 (Figure 3c), calculated from dune records from the central and northern dunefields.
463 Late Holocene dune records, however, remain scarce from the southern Thar
464 (Figure 1), with only 2 of the 18 luminescence ages from this area recording late
465 Holocene accumulation (Figure 1b). As the *AI* method focusses on the time period in
466 which sediments accumulated rather than treating individual ages as discrete dune
467 activity phases (Thomas and Bailey, 2017), peaks between ~3.5 and ~1.5 ka
468 suggest the beginning of a phase of accumulation instead of an activity phase.
469 Interestingly, the late Holocene, due to weakening of the ISM and reduced
470 monsoonal precipitation, represented a phase of pronounced aridity in the Thar. Jain
471 and Tandon (2003) and Jain et al. (2004), based on sedimentological analyses and
472 luminescence dating, suggested that the streams of rivers in the southern Thar
473 became defunct. Several lakes in the Thar like the Bap-Malar, Didwana,
474 Lunkaransar also showed high salinity levels or dried up during this phase (Wasson
475 et al., 1984; Singh et al., 1990; Kajale and Deotare, 1997; Deotare, 1998; Enzel et al.,

476 1999). Whilst the records of dune accumulation in the backdrop of weakening ISM
477 are sparse, the drying lakes and river sources acted as potential local sources of
478 sediment supply, and hence the *AI* peaks appear, even during a period of weakened
479 ISM intensity.

480 In Figure 3c, two *AI* peaks are observed: one centred around ~1 ka and the other
481 representing the recent century. In the last millennium, based on $\delta^{18}\text{O}$ values from a
482 speleothem from the Wah Shikar Cave in north-eastern India, it has been suggested
483 that ISM strength was variable, and coincided with intervals of droughts in the
484 subcontinent (Gupta et al., 2019). Other speleothem studies from the Dandak and
485 Jhumar Caves in central India (Sinha et al. 2007; Sinha et al., 2011a; Sinha et al.,
486 2011b; Berkelhammer et al., 2010) also reported weaker ISM conditions attributable
487 to drought conditions across large part of the country. In the Thar, there is recurring
488 evidence from different dune sites of continuous dune activity coinciding with some
489 of the historically reported long droughts. These droughts during 1255-1258, 1309-
490 1313, 1868-1870, 1899-1905 and 1935-39 have been attributed to weak and erratic
491 summer monsoons (Sharma 1966; Narain and Kar, 2005). The relationship between
492 drought events with dune activity has been investigated in some details in the
493 context of dunefields in the Kalahari (Thomas and Leason, 2005; Thomas and
494 Burrough, 2012) and the Nebraska Sandhills (Miao et al., 2007; Hanson et al., 2009;
495 Buckland et al., 2019) to demonstrate geomorphological consequences in the
496 landscape. It could be hypothesised that during drought events, vegetation covers on
497 dunes and groundwater levels fell affecting the stability of dunes and exposing their
498 surfaces to reactivation.

499 While a strengthening of the ISM in recent centuries has been suggested based on
500 marine productivity records (e.g. Anderson et al., 2002; Anderson et al., 2010) and

501 speleothem geochemistry from the Indian subcontinent (e.g. Gupta et al., 2019;
502 Sinha et al., 2011a), Gill et al. (2017) suggest that precipitation over northwest India
503 today is approximately 40% lower when compared to Early Holocene levels..
504 Instrumental meteorological data collection began during the mid-19th century in the
505 Thar Desert, and shows that fluctuations in rainfall inter-annually, but no long term
506 increase or decrease (Sontakke et al., 1993; Parthasarathy et al., 1994). From field
507 observations made throughout the year, Singhvi and Kar (2004) observed increased
508 levels of sand mobility in areas of significant human pressure, which they suggested
509 to be greater now than during the Late Quaternary period. This is seen in the strong
510 *AI* peaks in Figure 3c, which are comparable to the pronounced early Holocene *AI*
511 peaks, and are more likely to be the result of significant anthropogenic disturbances
512 in the Thar landscape. Since the subcontinent's independence seventy years ago,
513 the human population has seen a four-fold rise in the Thar as land reforms and the
514 construction of irrigation canals has increased access and agricultural potential (Kar
515 et al., 2014; Dhir, 2018). Today, the population density of the Thar is over 100
516 people/km² which surpasses not just other arid but many temperate regions too.
517 Increased livestock grazing, mechanised ploughing on dune slopes and excessive
518 groundwater pumping have all led to a significant deterioration in vegetation cover
519 and dune reactivation. Srivastava et al. (2019b) have shown that sensitive parabolic
520 dunes in the central Thar have recorded accumulation rates up to 5 m per year in the
521 recent century. Similar cases of anthropogenic drivers of dune activity have also
522 been observed in semi-arid regions of China (e.g. Yang et al., 2011; Xu et al., 2019;
523 Zhang and Huisingh, 2018) and the Negev (Tsoar, 2008; Roskin et al., 2013).

524

525

526 **4. Conclusions**

527 There are now more than 100 Holocene luminescence ages calculated from dunes
528 in the Thar Desert. This new *Al* analysis identifies multiple peaks of dune
529 accumulation, notably between ~12-~8 ka, and centred around ~7, ~5 and ~3.5 ka.
530 The strongest peaks are observed in recent centuries. The widespread early
531 Holocene dune accumulation is most likely to have occurred as a response to the
532 period of strengthened ISM that is recorded in the other proxies from the
533 subcontinent and beyond (e.g. Gupta et al., 2003; Fleitmann et al., 2003; Gill et al.,
534 2017). During the middle to late Holocene, when the ISM started to weaken
535 gradually, sediment supply facilitated by drying river channels in the northern Thar,
536 and anthropogenic disturbances in the central Thar have been significant drivers of
537 dune activity (e.g. Durcan et al., 2019; Srivastava et al., 2019b). The dune ages
538 cannot be translated simply to derive palaeoclimatic interpretation as they display a
539 nonlinear and complex relationship with rainfall and aridity, much like the dune
540 records from the Kalahari (Chase, 2009), the Arabia (Atkinson et al., 2011; Leighton
541 et al., 2014) and the Negev (Roskin et al., 2011). Thar fluvial and lacustrine records
542 also present a picture of dynamic yet divergent responses to drivers during the
543 Holocene. Along the northern margin of the Thar, the Ghaggar-Hakra system shows
544 a concurrence of fluvial and dune activities during the middle to late Holocene. The
545 lake records from the Thar also show complex relationships with ISM variations, and
546 it is therefore unsurprising that dune accumulation periods do not necessarily relate
547 to lake low phases. These complex geomorphic responses over time in the Thar,
548 and the lack of clear correlations between both lake/dune dynamics and ISM
549 changes inferred from marine records, indicates that landscape dynamics are likely
550 driven by the complex interplay of regional and more local drivers.

551 This study with the application of *AI* analysis, has allowed an enhanced recognition
552 of the complexity of landscape development in the Holocene. However, there still
553 remain challenges in constructing a holistic picture of landscape dynamics as the
554 Thar is under-sampled spatially and temporally with few intensive dunefield based
555 studies. Being an extensive desert with many distinct dune types, further dunefield
556 based studies are needed to represent the complexity of geomorphic evolution of the
557 Thar landscape through time.

558

559 **5. Acknowledgements**

560 The first author thanks the Clarendon Scholarship, University of Oxford for funding
561 his doctoral studies, and European Geosciences Union General Assembly 2019 and
562 INQUA Congress 2019 for supporting his attendance at these congresses where this
563 work was presented. The authors acknowledge all the people involved with the
564 papers cited herein for their time and efforts spent studying the region, and for the
565 data they have produced.

566

567

568

569

570

571

572

573 **References**

- 574 Allchin, B., Goudie, A. and Hegde, K., 1978. Prehistory and palaeogeography of the
575 Great Indian Desert.
- 576 Anderson, D.M., Baulcomb, C.K., Duvivier, A.K. and Gupta, A.K., 2010. Indian
577 summer monsoon during the last two millennia. *Journal of Quaternary Science*, 25(6),
578 pp.911-917.
- 579 Anderson, D.M., Overpeck, J.T. and Gupta, A.K., 2002. Increase in the Asian
580 southwest monsoon during the past four centuries. *Science*, 297(5581), pp.596-599.
- 581 Andrews, J.E., Singhvi, A.K., Kailath, A.J., Kuhn, R., Dennis, P.F., Tandon, S.K. and
582 Dhir, R.P., 1998. Do stable isotope data from calcrete record late Pleistocene
583 monsoonal climate variation in the Thar Desert of India? *Quaternary Research*, 50(3),
584 pp.240-251.
- 585 Atkinson, O.A., Thomas, D.S.G., Goudie, A.S. and Bailey, R.M., 2011. Late
586 Quaternary chronology of major dune ridge development in the northeast Rub'al-
587 Khali, United Arab Emirates. *Quaternary Research*, 76(1), pp.93-105.
- 588 Bailey, R.M. and Thomas, D.S.G., 2014. A quantitative approach to understanding
589 dated dune stratigraphies. *Earth Surface Processes and Landforms*, 39(5), pp.614-
590 631.
- 591 Band, S., Yadava, M.G., Lone, M.A., Shen, C.C., Sree, K. and Ramesh, R., 2018.
592 High-resolution mid-Holocene Indian Summer Monsoon recorded in a stalagmite
593 from the Kotumsar Cave, Central India. *Quaternary International*, 479, pp.19-24.
- 594 Berger, A. and Loutre, M.F., 1999. Parameters of the Earth's orbit for the last 5
595 Million years in 1 kyr resolution. PANGAEA.

596 Berkelhammer, M., Sinha, A., Mudelsee, M., Cheng, H., Edwards, R.L. and
597 Cannariato, K., 2010. Persistent multidecadal power of the Indian Summer Monsoon.
598 *Earth and Planetary Science Letters*, 290(1-2), pp.166-172.

599 Berkelhammer, M., Sinha, A., Stott, L., Cheng, H., Pausata, F.S. and Yoshimura, K.,
600 2012. An abrupt shift in the Indian monsoon 4000 years ago. *Geophys. Monogr.*
601 *Ser*, 198, pp.75-87.

602 Bowler, J.M., 1986. Spatial variability and hydrologic evolution of Australian lake
603 basins: analogue for Pleistocene hydrologic change and evaporite
604 formation. *Palaeogeography, Palaeoclimatology, Palaeoecology*, 54(1-4), pp.21-41.

605 Buckland, C.E., Thomas, D.S. and Bailey, R.M., 2019. Complex disturbance-driven
606 reactivation of near-surface sediments in the largest dunefield in North America
607 during the last 200 years. *Earth Surface Processes and Landforms*, 44(14), pp.2794-
608 2809.

609 Burrough, S.L. and Thomas, D.S.G., 2009. Geomorphological contributions to
610 palaeolimnology on the African continent. *Geomorphology*, 103(3), pp.285-298.

611 Chase, B., 2009. Evaluating the use of dune sediments as a proxy for palaeo-aridity:
612 a southern African case study. *Earth-Science Reviews*, 93(1-2), pp.31-45.

613 Cohen, A.S., 2003. *Paleolimnology: the history and evolution of lake systems.*
614 Oxford University Press.

615 Cohen, T.J., Nanson, G.C., Larsen, J.R., Jones, B.G., Price, D.M., Coleman, M. and
616 Pietsch, T.J., 2010. Late Quaternary aeolian and fluvial interactions on the Cooper
617 Creek Fan and the association between linear and source-bordering dunes,
618 Strzelecki Desert, Australia. *Quaternary Science Reviews*, 29(3-4), pp.455-471.

619 Deotare, B.C., Kajale, M.D., Kshirsagar, A.A. and Rajaguru, S.N., 1998.
620 Geoarchaeological and palaeoenvironmental studies around Bap–Malar playa,
621 district Jodhpur, Rajasthan. *Current Science*, pp.316-320.

622 Deotare, B.C., Kajale, M.D., Rajaguru, S.N., Kusumgar, S., Jull, A.T. and Donahue,
623 J.D., 2004. Palaeoenvironmental history of Bap-Malar and Kanod playas of western
624 Rajasthan, Thar desert. *Journal of Earth System Science*, 113(3), pp.403-425.

625 Dhir, R.P., Joshi, D.C. and Kathju, S., 2018. *Thar Desert in retrospect and prospect*.
626 Scientific Publishers.

627 Dhir, R.P., Singhvi, A.K., Andrews, J.E., Kar, A., Sareen, B.K., Tandon, S.K., Kailath,
628 A. and Thomas, J.V., 2010. Multiple episodes of aggradation and calcrete formation
629 in Late Quaternary aeolian sands, Central Thar Desert, Rajasthan, India. *Journal of*
630 *Asian Earth Sciences*, 37(1), pp.10-16.

631 Dixit, Y. and Tandon, S.K., 2016. Hydroclimatic variability on the Indian subcontinent
632 in the past millennium: review and assessment. *Earth-science reviews*, 161, pp.1-15.

633 Dixit, Y., Hodell, D.A. and Petrie, C.A., 2014a. Abrupt weakening of the summer
634 monsoon in northwest India~ 4100 yr ago. *Geology*, 42(4), pp.339-342.

635 Dixit, Y., Hodell, D.A., Giesche, A., Tandon, S.K., Gázquez, F., Saini, H.S., Skinner,
636 L.C., Mujtaba, S.A., Pawar, V., Singh, R.N. and Petrie, C.A., 2018. Intensified
637 summer monsoon and the urbanization of Indus Civilization in northwest
638 India. *Scientific reports*, 8(1), p.4225.

639 Dixit, Y., Hodell, D.A., Sinha, R. and Petrie, C.A., 2014b. Abrupt weakening of the
640 Indian summer monsoon at 8.2 kyr BP. *Earth and Planetary Science Letters*, 391,
641 pp.16-23.

642 Durcan, J.A., Thomas, D.S., Gupta, S., Pawar, V., Singh, R.N. and Petrie, C.A.,
643 2019. Holocene landscape dynamics in the Ghaggar-Hakra palaeochannel region at
644 the northern edge of the Thar Desert, northwest India. *Quaternary International*, 501,
645 pp.317-327.

646 Dutt, S., Gupta, A.K., Clemens, S.C., Cheng, H., Singh, R.K., Kathayat, G. and
647 Edwards, R.L., 2015. Abrupt changes in Indian summer monsoon strength during
648 33,800 to 5500 years BP. *Geophysical Research Letters*, 42(13), pp.5526-5532.

649 Enzel, Y., Ely, L.L., Mishra, S., Ramesh, R., Amit, R., Lazar, B., Rajaguru, S.N.,
650 Baker, V.R. and Sandler, A., 1999. High-resolution Holocene environmental changes
651 in the Thar Desert, northwestern India. *Science*, 284(5411), pp.125-128.

652 Fleitmann, D., Burns, S.J., Mangini, A., Mudelsee, M., Kramers, J., Villa, I., Neff, U.,
653 Al-Subbary, A.A., Buettner, A., Hippler, D. and Matter, A., 2007. Holocene ITCZ and
654 Indian monsoon dynamics recorded in stalagmites from Oman and Yemen
655 (Socotra). *Quaternary Science Reviews*, 26(1-2), pp.170-188.

656 Fleitmann, D., Burns, S.J., Mudelsee, M., Neff, U., Kramers, J., Mangini, A. and
657 Matter, A., 2003. Holocene forcing of the Indian monsoon recorded in a stalagmite
658 from southern Oman. *science*, 300(5626), pp.1737-1739.

659 Gill, E.C., Rajagopalan, B., Molnar, P.H., Kushnir, Y. and Marchitto, T.M., 2017.
660 Reconstruction of Indian summer monsoon winds and precipitation over the past
661 10,000 years using equatorial pacific SST proxy records. *Paleoceanography*, 32(2),
662 pp.195-216.

663 Giosan, L., Clift, P.D., Macklin, M.G., Fuller, D.Q., Constantinescu, S., Durcan, J.A.,
664 Stevens, T., Duller, G.A., Tabrez, A.R., Gangal, K. and Adhikari, R., 2012. Fluvial

665 landscapes of the Harappan civilization. Proceedings of the National Academy of
666 Sciences, 109(26), pp.E1688-E1694.

667 Goudie, A.S., Allchin, B. and Hegde, K.T.M., 1973. The former extensions of the
668 great Indian sand desert. Geographical Journal, pp.243-257.

669 Gupta, A.K., Anderson, D.M. and Overpeck, J.T., 2003. Abrupt changes in the Asian
670 southwest monsoon during the Holocene and their links to the North Atlantic
671 Ocean. Nature, 421(6921), p.354.

672 Gupta, A.K., Dutt, S., Cheng, H. and Singh, R.K., 2019. Abrupt changes in Indian
673 summer monsoon strength during the last~ 900 years and their linkages to socio-
674 economic conditions in the Indian subcontinent. Palaeogeography,
675 Palaeoclimatology, Palaeoecology, p.109347.

676 Hanson, P.R., Joeckel, R.M., Young, A.R. and Horn, J., 2009. Late Holocene dune
677 activity in the Eastern Platte River Valley, Nebraska. Geomorphology, 103(4),
678 pp.555-561.

679 Hesse, P.P., 2016. How do longitudinal dunes respond to climate forcing? Insights
680 from 25 years of luminescence dating of the Australian desert dunefields. Quaternary
681 International, 410, pp.11-29.

682 Ivanochko, T.S., Ganeshram, R.S., Brummer, G.J.A., Ganssen, G., Jung, S.J.,
683 Moreton, S.G. and Kroon, D., 2005. Variations in tropical convection as an amplifier
684 of global climate change at the millennial scale. Earth and Planetary Science
685 Letters, 235(1-2), pp.302-314.

686 Jain, M. and Tandon, S.K., 2003. Fluvial response to Late Quaternary climate
687 changes, western India. Quaternary Science Reviews, 22(20), pp.2223-2235.

688 Jain, M., Tandon, S.K. and Bhatt, S.C., 2004. Late Quaternary stratigraphic
689 development in the lower Luni, Mahi and Sabarmati river basins, western
690 India. *Journal of Earth System Science*, 113(3), pp.453-471.

691 Juyal, N., Kar, A., Rajaguru, S.N. and Singhvi, A.K., 2003. Luminescence chronology
692 of aeolian deposition during the Late Quaternary on the southern margin of Thar
693 Desert, India. *Quaternary International*, 104(1), pp.87-98.

694 Kajale, M.D. and Deotare, B.C., 1997. Late Quaternary environmental studies on salt
695 lakes in western Rajasthan, India: a summarised view. *Journal of Quaternary
696 Science: Published for the Quaternary Research Association*, 12(5), pp.405-412.

697 Kar, A., 1987. Origin and transformation of longitudinal sand dunes in the Indian
698 desert. *Zeitschrift fur Geomorphologie*, 31, pp.311-337.

699 Kar, A., 1993. Aeolian processes and bedforms in the Thar Desert. *Journal of Arid
700 Environments*, 25(1), pp.83-96.

701 Kar, A., 2014. The Thar or the Great Indian Sand Desert. In *Landscapes and
702 Landforms of India* (pp. 79-90). Springer, Dordrecht.

703 Kar, A., Felix, C., Rajaguru, S.N. and Singhvi, A.K., 1998. Late Holocene growth and
704 mobility of a transverse dune in the Thar Desert. *Journal of Arid Environments*, 38(2),
705 pp.175-185.

706 Kar, A., Singhvi, A.K., Rajaguru, S.N., Juyal, N., Thomas, J.V., Banerjee, D. and Dhir,
707 R.P., 2001. Reconstruction of the late Quaternary environment of the lower Luni
708 plains, Thar Desert, India. *Journal of Quaternary Science: Published for the
709 Quaternary Research Association*, 16(1), pp.61-68.

710 Kaushal, N., Breitenbach, S.F., Lechleitner, F.A., Sinha, A., Tewari, V.C., Ahmad,
711 S.M., Berkelhammer, M., Band, S., Yadava, M., Ramesh, R. and Henderson, G.M.,
712 2018. The Indian Summer Monsoon from a Speleothem $\delta^{18}\text{O}$ Perspective—A
713 Review. *Quaternary*, 1(3), p.29.

714 Kumar, A., Srivastava, P. and Meena, N.K., 2017. Late Pleistocene aeolian activity in
715 the cold desert of Ladakh: a record from sand ramps. *Quaternary International*, 443,
716 pp.13-28.

717 Lancaster, N., Wolfe, S., Thomas, D.S.G., Bristow, C., Bubbenzer, O., Burrough, S.L.,
718 Duller, G.A.T., Halfen, A., Hesse, P.P., Roskin, J. and Singhvi, A.K., 2016. The
719 INQUA dunes atlas chronologic database. *Quaternary international*, 410, pp.3-10.

720 Leighton, C.L., Bailey, R.M. and Thomas, D.S.G., 2014. Interpreting and modelling
721 late Quaternary dune accumulation in the southern Arabian Peninsula. *Quaternary*
722 *Science Reviews*, 102, pp.1-13.

723 Leipe, C., Demske, D., Tarasov, P.E. and Members, H.P., 2014. A Holocene pollen
724 record from the northwestern Himalayan lake Tso Moriri: implications for
725 palaeoclimatic and archaeological research. *Quaternary International*, 348, pp.93-
726 112.

727 Li, B. and Coulthard, T.J., 2015. Mapping the interactions between rivers and sand
728 dunes: implications for fluvial and aeolian geomorphology. *Geomorphology*, 231,
729 pp.246-257.

730 MacDonald, G., 2011. Potential influence of the Pacific Ocean on the Indian summer
731 monsoon and Harappan decline. *Quaternary International*, 229(1-2), pp.140-148.

732 Maemoku, H., Shitaoka, Y., Nagatomo, T. and Yagi, H., 2012. Geomorphological
733 constraints on the Ghaggar River regime during the Mature Harappan period. *Clim.*
734 *Landscapes Civilizations*, 198, pp.97-106.

735 Maroulis, J.C., Nanson, G.C., Price, D.M. and Pietsch, T., 2007. Aeolian–fluvial
736 interaction and climate change: source-bordering dune development over the past~
737 100 ka on Cooper Creek, central Australia. *Quaternary Science Reviews*, 26(3-4),
738 pp.386-404.

739 Miao, X., Mason, J.A., Swinehart, J.B., Loope, D.B., Hanson, P.R., Goble, R.J. and
740 Liu, X., 2007. A 10,000 year record of dune activity, dust storms, and severe drought
741 in the central Great Plains. *Geology*, 35(2), pp.119-122.

742 Misra, P., Tandon, S.K. and Sinha, R., 2019. Holocene climate records from lake
743 sediments in India: Assessment of coherence across climate zones. *Earth-science*
744 *reviews*, 190, pp.370-397.

745 Moharana, P.C., Gaur, M.C., Choudhary, C., Chauhan, J.S. and Rajpurohit, R.S.,
746 2013. A system of geomorphological mapping for western Rajasthan with relevance
747 for agricultural land use. *Annals of Arid Zone*, 52(3&4), pp.163-180.

748 Narain, P. and Kar, A., 2005. *Drought in Western Rajasthan*. ICAR-Central Arid Zone
749 Research Institute, Jodhpur.

750 Neff, U., Burns, S.J., Mangini, A., Mudelsee, M., Fleitmann, D. and Matter, A., 2001.
751 Strong coherence between solar variability and the monsoon in Oman between 9
752 and 6 kyr ago. *Nature*, 411(6835), p.290.

753 Parthasarathy, B., Munot, A.A. and Kothawale, D.R., 1994. All-India monthly and
754 seasonal rainfall series: 1871–1993. *Theoretical and Applied Climatology*, 49(4),
755 pp.217-224.

756 Ponton, C., Giosan, L., Eglinton, T.I., Fuller, D.Q., Johnson, J.E., Kumar, P. and
757 Collett, T.S., 2012. Holocene aridification of India. *Geophysical Research*
758 *Letters*, 39(3).

759 Prasad, S. and Enzel, Y., 2006. Holocene paleoclimates of India. *Quaternary*
760 *Research*, 66(3), pp.442-453.

761 Roskin, J., Katra, I. and Blumberg, D.G., 2013. Late Holocene dune mobilizations in
762 the northwestern Negev dunefield, Israel: A response to combined anthropogenic
763 activity and short-term intensified windiness. *Quaternary International*, 303, pp.10-23.

764 Roskin, J., Tsoar, H., Porat, N. and Blumberg, D.G., 2011. Palaeoclimate
765 interpretations of Late Pleistocene vegetated linear dune mobilization episodes:
766 evidence from the northwestern Negev dunefield, Israel. *Quaternary Science*
767 *Reviews*, 30(23-24), pp.3364-3380.

768 Saini, H. and Mujtaba, S., 2010. Luminescence dating of the sediments from a
769 buried channel loop in Fatehabad area, Haryana: insight into Vedic Saraswati River
770 and its environment. *Geochronometria*, 37(1), pp.29-35.

771 Sarkar, A., Ramesh, R., Somayajulu, B.L.K., Agnihotri, R., Jull, A.T. and Burr, G.S.,
772 2000. High resolution Holocene monsoon record from the eastern Arabian
773 Sea. *Earth and Planetary Science Letters*, 177(3-4), pp.209-218.

774 Sharma, D. ed., 1966. *Rajasthan Through the Ages: From the earliest times to 1316*
775 *AD (Vol. 1)*. Rajasthan State Archives.

776 Shitaoka, Y., Maemoku, H. and Nagatomo, T., 2012. Quartz OSL dating of sand
777 dunes in Ghaggar Basin, northwestern India. *Geochronometria*, 39(3), pp.221-226.

778 Singh, G., Wasson, R.J. and Agrawal, D.P., 1990. Vegetational and seasonal
779 climatic changes since the last full glacial in the Thar Desert, northwestern
780 India. *Review of Palaeobotany and Palynology*, 64(1-4), pp.351-358.

781 Singhvi, A.K. and Kar, A., 2004. The aeolian sedimentation record of the Thar
782 Desert. *Journal of Earth System Science*, 113(3), pp.371-401.

783 Singhvi, A.K. and Porat, N., 2008. Impact of luminescence dating on
784 geomorphological and palaeoclimate research in drylands. *Boreas*, 37(4), pp.536-
785 558.

786 Singhvi, A.K., Sharma, Y.P. and Agrawal, D.P., 1982. Thermoluminescence dating of
787 sand dunes in Rajasthan, India. *Nature*, 295(5847), p.313.

788 Sinha, A., Berkelhammer, M., Stott, L., Mudelsee, M., Cheng, H. and Biswas, J.,
789 2011a. The leading mode of Indian Summer Monsoon precipitation variability during
790 the last millennium. *Geophysical Research Letters*, 38(15).

791 Sinha, A., Cannariato, K.G., Stott, L.D., Cheng, H., Edwards, R.L., Yadava, M.G.,
792 Ramesh, R. and Singh, I.B., 2007. A 900-year (600 to 1500 AD) record of the Indian
793 summer monsoon precipitation from the core monsoon zone of India. *Geophysical
794 Research Letters*, 34(16).

795 Sinha, A., Stott, L., Berkelhammer, M., Cheng, H., Edwards, R.L., Buckley, B.,
796 Aldenderfer, M. and Mudelsee, M., 2011b. A global context for megadroughts in
797 monsoon Asia during the past millennium. *Quaternary Science Reviews*, 30(1-2),
798 pp.47-62.

799 Sinha, R., Smykatz-Kloss, W., Stüben, D., Harrison, S.P., Berner, Z. and Kramar, U.,
800 2006. Late Quaternary palaeoclimatic reconstruction from the lacustrine sediments
801 of the Sambhar playa core, Thar Desert margin, India. *Palaeogeography,*
802 *Palaeoclimatology, Palaeoecology*, 233(3-4), pp.252-270.

803 Sontakke, N.A., Pant, G.B. and Singh, N., 1993. Construction of all-India summer
804 monsoon rainfall series for the period 1844–1991. *Journal of Climate*, 6(9), pp.1807-
805 1811.

806 Srivastava, A., Durcan, J.A. and Thomas, D.S.G., 2019a. Analysis of late Quaternary
807 linear dune development in the Thar Desert, India. *Geomorphology*, 344, pp.90-98.

808 Srivastava, A., Thomas, D.S.G. and Durcan, J.A., 2019b. Holocene dune activity in
809 the Thar Desert, India. *Earth Surface Processes and Landforms*, 44(7), pp.1407-
810 1418.

811 Srivastava, P., Juyal, N., Singhvi, A.K., Wasson, R.J. and Bateman, M.D., 2001.
812 Luminescence chronology of river adjustment and incision of Quaternary sediments
813 in the alluvial plain of the Sabarmati River, north Gujarat, India. *Geomorphology*,
814 36(3-4), pp.217-229.

815 Staubwasser, M., Sirocko, F., Grootes, P.M. and Erlenkeuser, H., 2002. South Asian
816 monsoon climate change and radiocarbon in the Arabian Sea during early and
817 middle Holocene. *Paleoceanography*, 17(4), pp.15-1.

818 Thomas, D.S.G. and Bailey, R.M., 2017. Is there evidence for global-scale forcing of
819 Southern Hemisphere Quaternary desert dune accumulation? A quantitative method
820 for testing hypotheses of dune system development. *Earth Surface Processes and*
821 *Landforms*, 42(14), pp.2280-2294.

822 Thomas, D.S.G. and Bailey, R.M., 2019. Analysis of late Quaternary dunefield
823 development in Asia using the accumulation intensity model. *Aeolian Research*, 39,
824 pp.33-46.

825 Thomas, D.S.G. and Burrough, S.L., 2012. Interpreting geoproxies of late
826 Quaternary climate change in African drylands: implications for understanding
827 environmental change and early human behaviour. *Quaternary International*, 253,
828 pp.5-17.

829 Thomas, D.S.G. and Burrough, S.L., 2016. Luminescence-based dune chronologies
830 in southern Africa: analysis and interpretation of dune database records across the
831 subcontinent. *Quaternary International*, 410, pp.30-45.

832 Thomas, D.S.G. and Leason, H.C., 2005. Dunefield activity response to climate
833 variability in the southwest Kalahari. *Geomorphology*, 64(1-2), pp.117-132.

834 Thomas, J.V., Kar, A., Kailath, A.J., Juyal, N., Rajaguru, S.N. and Singhvi, A.K.,
835 1999. Late Pleistocene-Holocene-history of aeolian accumulation in the Thar Desert,
836 India. *Zeitschrift fur Geomorphologie Supplementband*, pp.181-194.

837 Tsoar, H., 2008. Land use and its effect on the mobilization and stabilization of the
838 north-western Negev sand dunes. In *Arid Dune Ecosystems* (pp. 79-89). Springer,
839 Berlin, Heidelberg.

840 Wang, Y., Cheng, H., Edwards, R.L., He, Y., Kong, X., An, Z., Wu, J., Kelly, M.J.,
841 Dykoski, C.A. and Li, X., 2005. The Holocene Asian monsoon: links to solar changes
842 and North Atlantic climate. *Science*, 308(5723), pp.854-857.

843 Wasson, R.J., Rajaguru, S., Misra, V.N., Agrawal, D.P. and Dhir, R.P., 1983.
844 Geomorphology, late Quaternary stratigraphy and paleoclimatology of the Thar
845 dunefield. *Zeitschrift für Geomorphologie. Supplementband*, 45, pp.117-151.

846 Wasson, R.J., Smith, G.I. and Agrawal, D.P., 1984. Late Quaternary sediments,
847 minerals, and inferred geochemical history of Didwana Lake, Thar Desert,
848 India. *Palaeogeography, Palaeoclimatology, Palaeoecology*, 46(4), pp.345-372.

849 Xu, D., You, X. and Xia, C., 2019. Assessing the spatial-temporal pattern and
850 evolution of areas sensitive to land desertification in North China. *Ecological*
851 *indicators*, 97, pp.150-158.

852 Yadava, M.G. and Ramesh, R., 1999. Speleothems—useful proxies for past
853 monsoon rainfall.

854 Yang, X., Liu, T. and Xiao, H., 2003. Evolution of megadunes and lakes in the
855 Badain Jaran Desert, Inner Mongolia, China during the last 31,000
856 years. *Quaternary International*, 104(1), pp.99-112.

857 Yang, X., Ma, N., Dong, J., Zhu, B., Xu, B., Ma, Z. and Liu, J., 2010. Recharge to the
858 inter-dune lakes and Holocene climatic changes in the Badain Jaran Desert, western
859 China. *Quaternary Research*, 73(1), pp.10-19.

860 Yang, X., Scuderi, L., Paillou, P., Liu, Z., Li, H. and Ren, X., 2011. Quaternary
861 environmental changes in the drylands of China—a critical review. *Quaternary*
862 *Science Reviews*, 30(23-24), pp.3219-3233.

863 Zhang, Z. and Huisin, D., 2018. Combating desertification in China: Monitoring,
864 control, management and revegetation. *Journal of cleaner production*, 182, pp.765-
865 775.